Site Isolation in Metal-Organic Layers Enhances Photoredox Gold Catalysis

Haifeng Zheng,[#] Yingjie Fan,[#] Yang Song, Justin S. Chen, Eric You, Steven Labalme, and Wenbin Lin*

Department of Chemistry, The University of Chicago, Chicago, Illinois 60637, United States

ABSTRACT: Herein, we report the synthesis of a metal−organic layer, Hf-Ru-Au, containing Ru(bipyridine)$_3^{2+}$-type photosensitizers and (phosphine)-AuCl catalysts for photoredox Au-catalyzed cross-coupling of allenoates, alkenes, or alkynes with aryldiazonium salts to afford furanone, tetrahydrofuran, or aryl alkyne derivatives, respectively. Site isolation of (phosphine)-AuCl complexes in Hf-Ru-Au prevents Au catalyst deactivation via ligand redistribution, Au(I) disproportionation, and aryl-phosphine reductive elimination while the proximity between Ru photosensitizers and Au catalysts enhances catalytic efficiency, with 14-200 times higher activity over the homogeneous controls in the cross-coupling reactions.

Gold (Au) catalysts are widely used in various transformations of C-C multiple bonds, including hydrofunctionalization and difunctionalization of alkenes, alkynes, and allenes.[1-3] In these reactions, Au complexes serve as soft π-Lewis acids to activate unsaturated C-C bonds for nucleophilic additions. Au complexes can also catalyze cross-coupling reactions in the presence of strong oxidants.[4] In 2013, Glorius and coworkers merged photoredox catalysis with Au catalysis to mediate the Au(I)/Au(III) cycle for oxy- and aminoarylation of alkenes.[5] Photoredox Au catalysis has provided powerful methods for the difunctionalization of π-systems.[6-9]

Homogeneous Au-catalyzed reactions typically require high catalyst loadings (1-10 mol%) due to relatively low reactivity of Au complexes and rapid catalyst deactivation.[10-11] Hammond, Xu, and coworkers proposed the deactivation of Au catalysts via a ligand redistribution to form bis(phosphine)-Au(I) and non-coordinated Au(I) compounds, followed by disproportionation of non-coordinated Au(I) compounds into Au(III) species and catalytically-inactive Au(0) nanoparticles.[11, 12] The (aryl)(phosphine)gold intermediate can also undergo aryl-phosphine reductive elimination to deactivate gold catalysts.[13] While Au catalysts have been used in total synthesis[14-15] and material design,[16-18] catalyst deactivation presents a hurdle to broader application of Au catalysis.

Metal-organic frameworks (MOFs) have provided a versatile platform for studying single-site catalysis.[19-27] Incorporation of metal catalysts into MOFs creates site-isolated metal centers, which prevents catalyst deactivation via disproportionation pathways.[28] Au(I) centers were previously incorporated into a phosphine-containing MOF for the hydroaddition of 4-pentyn-1-ol.[21]

Although MOFs can be functionalized to afford single-site catalysts,[19, 29-31] it is challenging to incorporate multiple distinct active sites into MOFs.[32-38] We have recently developed two-dimensional metal-organic layers (MOLs) for tandem and photoredox catalysis.[39-42] Unlike MOFs, MOLs have completely accessible and modifiable ligands and SBUs to allow hierarchical integration of distinct active sites. The proximity between different active sites in MOLs further enhances their catalytic efficiency. We hypothesized that MOLs could hierarchically integrate photosensitizers and Au catalysts to not only prevent Au catalyst deactivation but also enhance photoredox catalytic activities with proximately placed photosensitizers and Au(I) complexes (Figure 1).

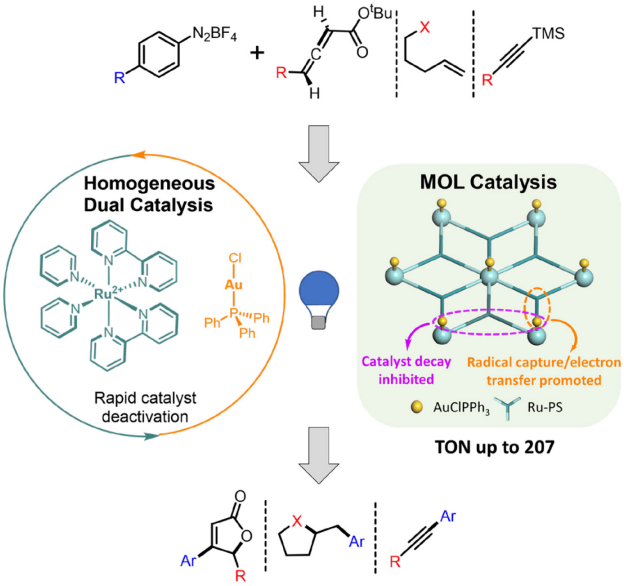

Figure 1. Schematic showing homogeneous dual catalysis and MOL-supported site-isolated Au complexes for photoredox cross-coupling reactions.

In this work, we synthesized a new Hf-Ru-Au MOL containing Ru((BPY)(bpy)$_2^{2+}$ (BPY = 4',6'-dibenzoato-[2,2'-bipyridine]-4-carboxylate) photosensitizers (Ru-PSs) and (phosphine)-AuCl complexes for photoredox catalysis. Hf-BPY MOL was first built from Hf_6 SBUs and BPY bridging ligands. Postsynthetic modification of Hf_6-BPY allowed the installation of Ru-PSs on BPY ligands and (4-(diphenylphosphino)phenyl acetic acid)-Au(I) chloride (**P**-AuCl) on Hf_6 SBUs to afford Hf-Ru-Au, which showed 14- to 200-fold higher catalytic activities over homogeneous controls in cross-coupling reactions of allenoates, alkenes, or alkynes with aryldiazonium salts to afford

furanone, tetrahydrofuran, or aryl alkyne derivatives, respectively.

The synthesis of Hf-Ru-Au started from a solvothermal reaction of $HfCl_4$ and H_3BPY in dimethylformamide with formic acid and water at 120 ºC to afford the known Hf-BPY MOL with a formula of $Hf_6(\mu_3\text{-}O)_4(\mu_3\text{-}OH)_4(BPY)_2(HCO_2)_6$ (Figure 2a).[43] Hf-BPY was treated with $Ru(bpy)_2Cl_2$ at 80 ºC for two days to yield Hf-Ru MOL by partially metalating bipyridine sites in Hf-BPY. Subsequent reaction of Hf-Ru with **P**-AuCl in acetonitrile at 60 ºC afforded Hf-Ru-Au by partially replacing formate capping groups on Hf_6 SBUs in Hf-Ru with **P**-AuCl (Figure 2a).

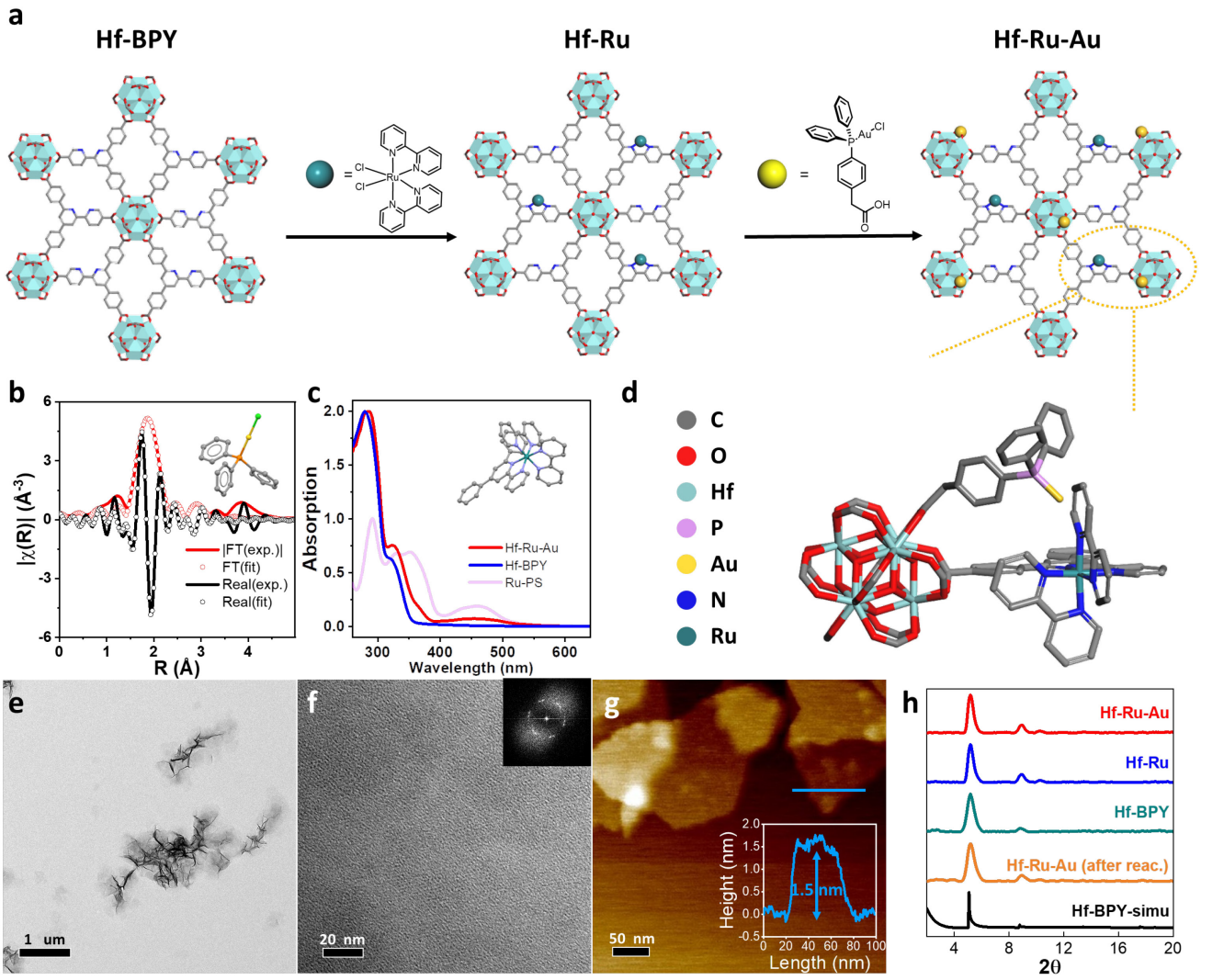

Figure 2. Synthesis and characterization of Hf-Ru-Au. (a) Schematic showing the synthesis of Hf-Ru-Au. (b) EXAFS fitting of Au in Hf-Ru-Au. The structure of $(PPh_3)AuCl$ is shown in the inset. (c) UV-vis spectra of Hf-Ru-Au, Hf-BPY and Ru-PS. The structure of Ru-PS is shown in the inset. (d) Stick model showing the attachment of **P**-AuCl and Ru-PS to a Hf_6 SBU. (e) TEM image, (f) HRTEM image (FFT pattern in the inset), (g) AFM image (height profile in the inset) of Hf-Ru-Au. (h) PXRD patterns of Hf-Ru-Au, Hf-Ru, Hf-BPY, Hf-Ru-Au after a catalytic reaction, and simulated PXRD pattern of Hf-BPY.

Inductively coupled plasma-mass spectrometry (ICP-MS) measurements showed a Hf : Ru : Au molar ratio of 6 : 0.32 : 0.50 for Hf-Ru-Au. Extended X-ray absorption fine structure (EXAFS) analysis revealed that Hf-Ru-Au had a similar Au(I) coordination environment to $(PPh_3)AuCl$ with Au-P and Au-Cl distances of 2.31 and 2.22 Å, respectively (Figure 2b). The UV-vis spectrum of Hf-Ru-Au showed additional peaks at 350 nm and 460 nm over Hf-BPY (Figure 2c), indicating the installation of Ru-PSs. ^1H and ^{31}P NMR spectra of digested Hf-Ru-Au showed signals of BPY, Ru-PS, and **P**-AuCl (Figure S11, S12). These results support the successful integration of Ru-PSs and Au catalysts into Hf-Ru-Au (Figure 2d) to afford an empirical formula of $Hf_6(\mu_3\text{-}O)_4(\mu_3\text{-}OH)_4(BPY)_{1.68}(Ru(bpy)_2BPY)_{0.32}(HCO_2)_{5.5}(\mathbf{P}\text{-}AuCl)_{0.5}$.

Transmission electron microscopy (TEM) showed a similar ruffled nanosheet morphology for Hf-BPY, Hf-Ru, and Hf-Ru-Au (Figure 2e, Figure S10). High-resolution TEM image of Hf-Ru-Au revealed a regular lattice structure with its fast Fourier transform (FFT) showing a hexagonal symmetry corresponding to the 2-D MOL structure (Figure 2f). The thickness of Hf-Ru-Au nanosheets was measured to be 1.5 nm by atomic force microscopy (AFM), corresponding to the height of a modified Hf_6 cluster (Figure 2g, S15).[42] Hf-BPY, Hf-Ru, and Hf-Ru-Au showed similar powder X-ray diffraction (PXRD) patterns that matched the simulated pattern of Hf-BPY (Figure 2h). These

results indicated that Hf-Ru-Au retained the structure of Hf-BPY after post-synthetic modifications. In Hf-Ru-Au, 8% of formate groups were replaced by **P**-AuCl and 16% of BPY ligands were metalated with $Ru(bpy)_2Cl_2$.

With installed Ru-PSs and Au catalysts, Hf-Ru-Au competently mediated dual photodedox and Au catalysis. The photocatalytic performance of Hf-Ru-Au was evaluated in three important cross-coupling reactions, including cross-coupling of allenoates, alkenes, and alkynes with aryldiazonium salts under mild conditions (visible light and room temperature).[3-4,7-8, 44-45]

As shown in Table 1a, 0.6 mol% Hf-Ru-Au efficiently catalyzed cross-coupling of allenoates with aryldiazonium salts to afford furanone derivatives. Substituents on allenoates (**2**), such as methyl (**2a**), isopropyl (**2b**) and benzyl (**2d**) groups were tolerated in the reactions to furnish the corresponding products **3a**, **3b** and **3d** in 78-81% yields. Homopropargyl allenoate (**2c**) also reacted with phenyldiazonium salt (**1a**) to afford **3c** in 55% yield. Both electron-donating (**1b**) and electron-withdrawing (**1c-1f**) substituents on aryldiazonium salts were tolerated in these reactions to form **3e-3h** in 65-83% yields.

Hf-Ru-Au at a 0.7 mol % catalyst loading catalyzed intermolecular oxy- and aminoarylation of alkenes and aryldiazonium salts to produce tetrahydrofuran and pyrrolidine derivates (Table 1b). Homoallylic alcohol (**4a**) and sulfonamide (**4b**) reacted with **1a** to afford tetrahydrofuran product **5a** and pyrrolidine product **5b** in 60% and 55% yields, respectively. The oxyarylation process worked with a diverse range of substituted aryldiazonium salts **1b-1g** to yield the corresponding tetrahydrofuran derivatives **5c-5g** in 45-70% isolated yields. Aryldiazonium salts bearing electron-withdrawing substituents (**1c-1e**) had higher yields than those with electron-donating groups (**1b** and **1f**).

Hf-Ru-Au at a 0.7 mol % catalyst loading also catalyzed cross-coupling of aryldiazonium salts (**1**) and arylethynylsilanes (**6**, Table 1c). Aryldiazonium salts with various substituents (**1a-1f**) reacted with **6a** to furnish aryl alkynes **7a-7f** in 36-70% yields**.** Electron-rich aryldiazonium **1b** gave a lower yield than electron-poor aryldiazoniums **1c-1f**, likely due to the competitive generation of aryl cations through loss of dinitrogen in **1b**. Arylethynylsilanes with both electron-withdrawing 4-chloro (**6b**) and electron-donating 4-methyl (**6c**) substituents reacted with **1c** to afford **7g** and **7h** in 72% and 75% yields, respectively. It is worth noting that the coupling reaction tolerates aryldiazonium salts and arylethynylsilanes with halogen substituents which allow for further functionalization.

Table 1. Hf-Ru-Au-catalyzed cross-coupling reactions of allenoates, alkenes, or alkynes with aryldiazonium salts.[a]

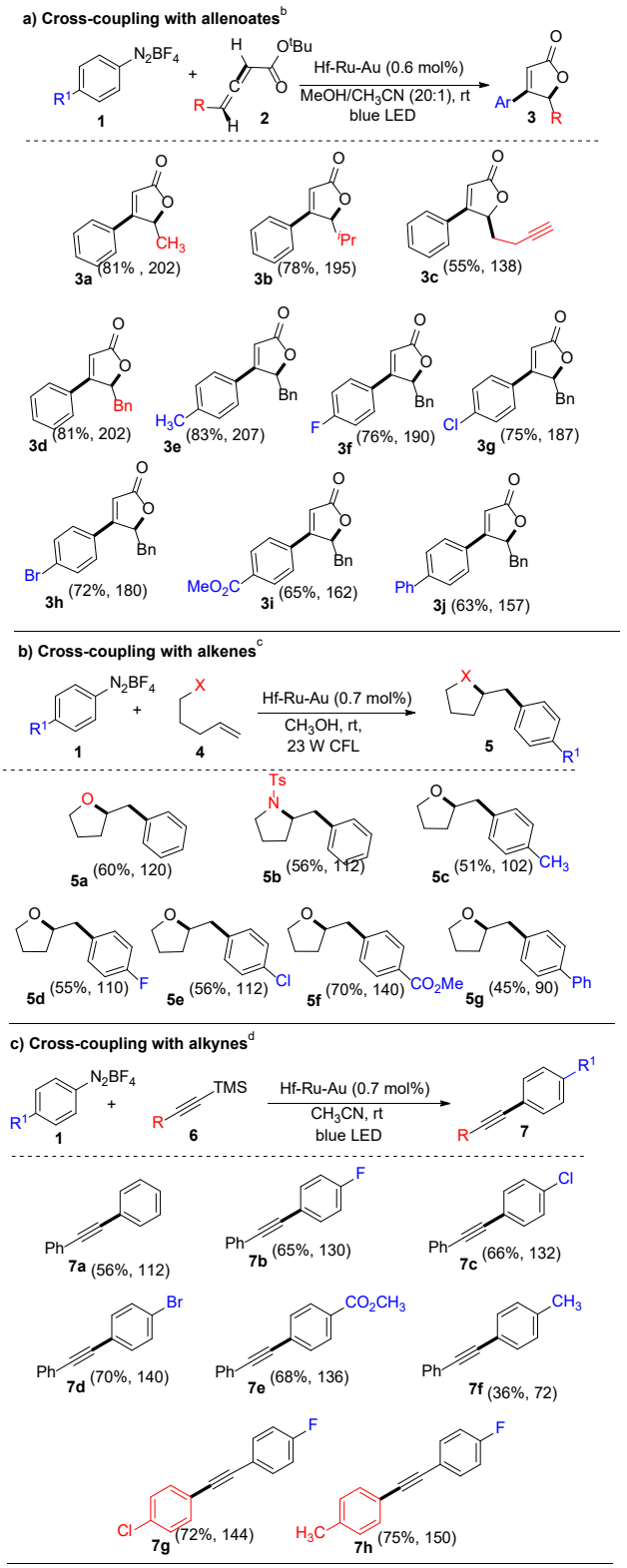

[a]Isolated yields and TONs are shown in parentheses and all reactions were performed at rt for 12 h. Catalyst loadings were based on Au. [b]**2** (0.2 mmol), **1** (0.8 mmol) and Hf-Ru-Au (0.6 mol %) in CH_3OH/CH_3CN. [c]**4** (0.2 mmol), **1** (0.8 mmol), and Hf-Ru-Au (0.7 mol %) in CH_3OH. [d]**6** (0.2 mmol), **1** (0.4 mmol) and Hf-Ru-Au (0.7 mol %) in CH_3CN.

We performed several control reactions to reveal the mechanism of Hf-Ru-Au catalyzed cross-coupling reactions. With alkyne **6a** as substrate, a homogeneous mixture of Ru-PS and **P**-AuCl in a 1:1.5 molar ratio afforded cross-coupled products in low yields (Table 2, entry 2). Seven-fold higher **P**-AuCl and 2-fold higher Ru-PS were needed to afford the cross-coupled product in a comparable yield as Hf-Ru-Au (Table 2, entry 3), indicating that Hf-Ru-Au is approximately 14 times more active than the homogeneous control. When allenoate **2d** or alkene **4a** was used as substrate, Hf-Ru-Au showed 200- or 140-fold higher activity, respectively, than the corresponding homogeneous control (Table S3). MOLs loaded with Ru-PS only (Hf-Ru) or **P**-AuCl only (Hf-Au) afforded the cross-coupling product **7b** in trace or 14% yields, respectively (Table 2, entry 4 and 5). The latter likely resulted from a radical chain process.[46] Hf-Ru-Au failed to catalyze the reaction in the absence of light (Table 2, entry 6). These results indicate the photoredox nature of the reaction and its dependence on the cooperativity between Ru-PS and **P**-AuCl.

Table 2. Control experiments of Hf-Ru-Au catalyzed cross-coupling reactions.[a]

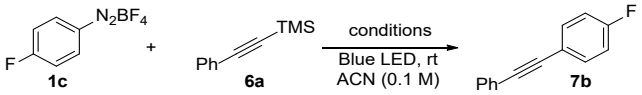

Entry	Catalyst(s)[b]	Yield (**7b**)
1	0.7 mol% Hf-Ru-Au	65%
2	0.5 mol% Ru-PS, 0.7 mol% **P**-AuCl	8%
3	1 mol% Ru-PS, 5 mol% **P**-AuCl	68%
4[b]	0.5 mol% Hf-Ru	0
5	0.7 mol% Hf-Au	14
6[c]	0.7 mol% Hf-Ru-Au	0

[a]Reactions were conducted with **6a** (0.2 mmol), **1c** (0.4 mmol) and the catalyst loadings were based on Au. [b]Catalyst loading was based on Ru. [c]Without blue LED irradiation.

Hf-Ru-Au catalyzed all three cross-coupling reactions with very low catalyst loadings of 0.6-0.7 mol %. In contrast, homogeneous dual photoredox and Au catalysis processes typically required 5-10 mol% Au catalysts. [3-4,7-8, 44-45] We attributed this large difference in catalytic activity to two factors: the proximity between Ru-PSs and Au catalysts (with the shortest distance of 0.7 nm, Figure 2d, S15) which facilitates the transfer of electron and radical intermediates[39] and the isolation of Au catalysts which prevent their deactivation via ligand redistribution, Au(I) disproportionation, and aryl-phosphine reductive elimination.

To understand the effect of Au(I) site isolation on the catalytic reactions, we examined the reaction mixtures of **1c** and **6a** with Hf-Ru-Au or homogeneous catalysts at 12 h by ^{31}P NMR. The ^{31}P NMR spectra of **P**-AuCl and digested Hf-Ru-Au (0 h) were collected for comparison (Figure 3a). The **P**-AuCl complex in Hf-Ru-Au remained unchanged with a peak at δ32.6 throughout the photocatalytic reaction. PXRD studies demonstrated the structural stability of Hf-Ru-Au MOL during the reaction (Figure 2h). When higher loadings of homogeneous catalysts were used to afford cross-coupled products in reasonable yields, we observed complete disappearance of **P**-AuCl and the formation of the phenyl-phosphonium salt with a ^{31}P NMR peak at δ 22.9 and a characteristic high-resolution MS peak for [$\mathbf{P}_2$-Au]$^+$. We believe that the phenyl-phosphonium salt likely results from reductive elimination from the putative $\mathbf{P}_2$-Au-aryl intermediate (Figure 3b, side reaction).[10, 47-48]

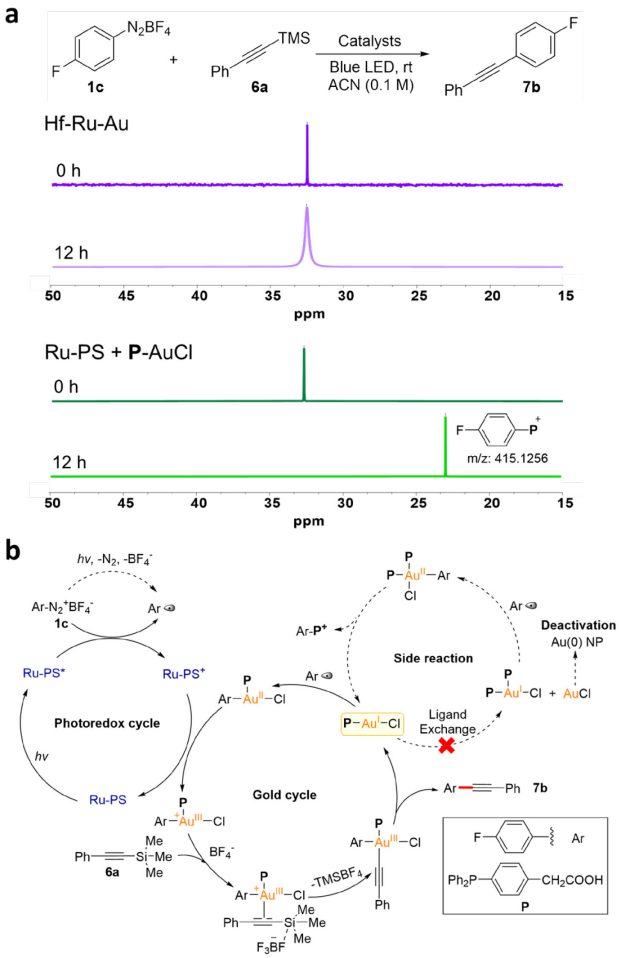

Figure 3. (a) ^{31}P NMR study of cross-coupling reaction mixtures between **1c** and **6a**. (b) Proposed mechanism for Hf-Ru-Au catalyzed cross-coupling reaction between **1c** and **6a**.

In support of this hypothesis, a mixture of Ru-PS and $\mathbf{P}_2$-AuCl competently catalyzed cross-coupling of **1c** and **6a** to afford **7b** in a comparable yield to the reaction catalyzed by Ru-PS and **P**-AuCl. Neither $\mathbf{P}_2$-Au complex nor phenyl-phosphonium salt was observed during Hf-Ru-Au catalyzed reactions. We believe that the isolation of Au(I) sites in Hf-Ru-Au shuts down the ligand redistribution and Au(I) disproportionation pathway as well as preventing the formation of the $\mathbf{P}_2$-Au-aryl intermediate and hence the phenyl-phosphonium byproduct (Figure 3b, side reaction). Consequently, the catalytic activity of Hf-Ru-Au was maintained throughout the reactions, which was demonstrated by recovery and reuse of Hf-Ru-Au in three runs of cross-coupling between **1c** and **6a**, with no decrease in catalytic activity. Leaching of Hf, Ru, and Au in the first cycle was determined by ICP-MS to be <0.5%, <0.5% and <1.6%, respectively (Table S1).

Based on these results and literature precedents,[6, 10, 49-53] we propose a plausible mechanism for Hf-Ru-Au catalyzed cross-coupling in Figure 3b. Aryldiazonium salt **1c** is reduced by excited Ru-PS or initiated by a light-mediated radical chain process to generate an aryl radical, which adds to **P**-AuCl and forms an Au(II)-aryl complex. The Au(II) complex is oxidized by [Ru-PS]$^+$ to Au(III). After coordination of Au(III) with alkyne **6a**

and fluorine anion-assisted desilylation, reductive elimination of the Au(III)-(aryl)(alkynyl) intermediate afforded product **7b** and regenerated the **P**-AuCl catalyst. Due to site isolation of **P**-AuCl species and synergistic effect between Ru-PS and **P**-AuCl, Hf-Ru-Au effectively shuts down the side reaction pathway in Figure 3b and enhances catalytic activity by 14-200 times.

In summary, we have designed a new bifunctional MOL, Hf-Ru-Au, containing $Ru(bpy)_3^{2+}$-type photosensitizer and **P**-AuCl catalyst. Hf-Ru-Au effectively catalyzed photoredox cross-coupling reactions alkenes, allenoates, or alkynes with aryldiazonium salts to afford furanone, tetrahydrofuran, and aryl alkyne derivatives with turnover numbers of up to 207. Hf-Ru-Au outperformed homogeneous controls by 14-200 times owing to site isolation of Au(I) and proximity of Ru-PS and Au catalyst. This work highlights the potential of MOLs as an excellent platform for developing synergistic photoredox catalysts with enhanced activities.

ASSOCIATED CONTENT

The supporting information is available free of charge on the ACS Publication website at

Materials and methods, synthesis and Characterization of 4-(Diphenylphosphino)phenylacetic Acid and Its Gold(I) Complex, synthesis and characterization of Hf-Ru-Au MOL, catalytic reactions and characterization of products, control experiments, mechanistic study, NMR spectra.

AUTHOR INFORMATION

Corresponding Author

Wenbin Lin − *Department of Chemistry, The University of Chicago, Chicago, Illinois 60637, United States*;
orcid.org/0000-0001-7035-7759;
Email: wenbinlin@uchicago.edu

Other Authors

Haifeng Zheng – *Department of Chemistry, The University of Chicago, Chicago, Illinois 60637, United States*;

orcid.org/0000-0002-1459-7253

Yingjie Fan − *Department of Chemistry, The University of Chicago, Chicago, Illinois 60637, United States*;

orcid.org/0000-0003-1857-5788

Yang Song − *Department of Chemistry, The University of Chicago, Chicago, Illinois 60637, United States*;

orcid.org/0000-0003-4212-8814

Justin S. Chen - *Department of Chemistry, The University of Chicago, Illinois 60637, United States*;

orcid.org/0000-0003-0192-3125

Eric You − *Department of Chemistry, The University of Chicago, Chicago, Illinois 60637, United States*;

orcid.org/0000-0002-5620-4083

Steven Labalme − *Department of Chemistry, The University of Chicago, Chicago, Illinois 60637, United States.*

Author Contributions

[#] H.Z. and Y.F. contributed equally.

Notes

The authors declare no competing financial interest.

ACKNOWLEDGMENT

We thank Xiaomin Jiang for experimental help. We acknowledge the National Science Foundation (CHE-2102554) and the University of Chicago for funding support and the MRSEC Shared User Facilities at the University of Chicago (DMR-1420709) for instrument Access. XAS analysis was performed at Beamline 10-BM, supported by the Materials Research Collaborative Access Team (MRCAT). Use of the Advanced Photon Source, an Office of Science User Facility operated for the U.S. DOE Office of Science by ANL, was supported by the U.S. DOE under Contract DE-AC02-06CH11357.

REFERENCES

1. Hashmi, A. S. K., Gold-Catalyzed Organic Reactions. *Chem. Rev.* **2007,** *107* (7), 3180-3211.
2. Zheng, Z.; Ma, X.; Cheng, X.; Zhao, K.; Gutman, K.; Li, T.; Zhang, L., Homogeneous Gold-Catalyzed Oxidation Reactions. *Chem. Rev.* **2021,** *121* (14), 8979-9038.
3. Michelet, V.; Toste, F. D., *Gold catalysis : an homogeneous approach / edited by F. Dean Toste, Veronique Michelet*. Imperial College Press: London, England, 2014.
4. Zhang, G.; Cui, L.; Wang, Y.; Zhang, L., Homogeneous Gold-Catalyzed Oxidative Carboheterofunctionalization of Alkenes. *J. Am. Chem. Soc.* **2010,** *132* (5), 1474-1475.
5. Sahoo, B.; Hopkinson, M. N.; Glorius, F., Combining Gold and Photoredox Catalysis: Visible Light-Mediated Oxy- and Aminoarylation of Alkenes. *J. Am. Chem. Soc.* **2013,** *135* (15), 5505-5508.
6. Hopkinson, M. N.; Tlahuext-Aca, A.; Glorius, F., Merging Visible Light Photoredox and Gold Catalysis. *Acc. Chem. Res.* **2016,** *49* (10), 2261-2272.
7. Tlahuext-Aca, A.; Hopkinson, M. N.; Sahoo, B.; Glorius, F., Dual gold/photoredox-catalyzed C(sp)–H arylation of terminal alkynes with diazonium salts. *Chem. Sci.* **2016,** *7* (1), 89-93.
8. He, Y.; Wu, H.; Toste, F. D., A dual catalytic strategy for carbon–phosphorus cross-coupling via gold and photoredox catalysis. *Chem. Sci.* **2015,** *6* (2), 1194-1198.
9. Witzel, S.; Hashmi, A. S. K.; Xie, J., Light in Gold Catalysis. *Chem. Rev.* **2021,** *121* (14), 8868-8925.
10. Cai, R.; Lu, M.; Aguilera, E. Y.; Xi, Y.; Akhmedov, N. G.; Petersen, J. L.; Chen, H.; Shi, X., Ligand-Assisted Gold-Catalyzed Cross-Coupling with Aryldiazonium Salts: Redox Gold Catalysis without an External Oxidant. *Angew. Chem. Int. Ed.* **2015,** *54* (30), 8772-8776.
11. Lu, Z.; Hammond, G. B.; Xu, B., Improving Homogeneous Cationic Gold Catalysis through a Mechanism-Based Approach. *Acc. Chem. Res.* **2019,** *52* (5), 1275-1288.
12. Sinha, P.; Wilson, A. K.; Omary, M. A., Beyond a T-Shape. *J. Am. Chem. Soc.* **2005,** *127* (36), 12488-12489.
13. Kawai, H.; Wolf, W. J.; DiPasquale, A. G.; Winston, M. S.; Toste, F. D., Phosphonium Formation by Facile Carbon–Phosphorus Reductive Elimination from Gold(III). *J. Am. Chem. Soc.* **2016,** *138* (2), 587-593.
14. Pflästerer, D.; Hashmi, A. S. K., Gold catalysis in total synthesis – recent achievements. *Chem. Soc. Rev.* **2016,** *45* (5), 1331-1367.
15. Rudolph, M.; Hashmi, A. S. K., Gold catalysis in total synthesis—an update. *Chem. Soc. Rev.* **2012,** *41* (6), 2448-2462.
16. Hendrich, C. M.; Sekine, K.; Koshikawa, T.; Tanaka, K.; Hashmi, A. S. K., Homogeneous and Heterogeneous Gold Catalysis for Materials Science. *Chem. Rev.* **2021,** *121* (14), 9113-9163.
17. Stuck, F.; Dietl, M. C.; Meißner, M.; Sebastian, F.; Rudolph, M.; Rominger, F.; Krämer, P.; Hashmi, A. S. K., Modular Two-Step Access to π-Extended Naphthyridine Systems—Potent Building Blocks for Organic Electronics. *Angew. Chem. Int. Ed.* **2022,** *61* (4), e202114277.
18. Heckershoff, R.; Schnitzer, T.; Diederich, T.; Eberle, L.; Krämer, P.; Rominger, F.; Rudolph, M.; Hashmi, A. S. K., Efficient Synthesis of Dipyrrolobenzenes and Dipyrrolopyrazines via Bidirectional Gold Catalysis: a Combined Synthetic and Photophysical Study. *J. Am. Chem. Soc.* **2022,** *144* (18), 8306-8316.

19. Drake, T.; Ji, P.; Lin, W., Site Isolation in Metal–Organic Frameworks Enables Novel Transition Metal Catalysis. *Acc. Chem. Res.* **2018,** *51* (9), 2129-2138.

20. Sun, C.; Skorupskii, G.; Dou, J.-H.; Wright, A. M.; Dincă, M., Reversible Metalation and Catalysis with a Scorpionate-like Metallo-ligand in a Metal–Organic Framework. *J. Am. Chem. Soc.* **2018,** *140* (50), 17394-17398.

21. Dunning, S. G.; Nandra, G.; Conn, A. D.; Chai, W.; Sikma, R. E.; Lee, J. S.; Kunal, P.; Reynolds Iii, J. E.; Chang, J.-S.; Steiner, A.; Henkelman, G.; Humphrey, S. M., A Metal–Organic Framework with Cooperative Phosphines That Permit Post-Synthetic Installation of Open Metal Sites. *Angew. Chem. Int. Ed.* **2018,** *57* (30), 9295-9299.

22. Mon, M.; Ferrando-Soria, J.; Grancha, T.; Fortea-Pérez, F. R.; Gascon, J.; Leyva-Pérez, A.; Armentano, D.; Pardo, E., Selective Gold Recovery and Catalysis in a Highly Flexible Methionine-Decorated Metal–Organic Framework. *J. Am. Chem. Soc.* **2016,** *138* (25), 7864-7867.

23. Lee, J. S.; Kapustin, E. A.; Pei, X.; Llopis, S.; Yaghi, O. M.; Toste, F. D., Architectural Stabilization of a Gold(III) Catalyst in Metal-Organic Frameworks. *Chem* **2020,** *6* (1), 142-152.

24. Furukawa, H.; Cordova, K. E.; O'Keeffe, M.; Yaghi, O. M., The Chemistry and Applications of Metal-Organic Frameworks. *Science* **2013,** *341* (6149), 974-974.

25. Liang, J.; Chen, R.-P.; Wang, X.-Y.; Liu, T.-T.; Wang, X.-S.; Huang, Y.-B.; Cao, R., Postsynthetic ionization of an imidazole-containing metal–organic framework for the cycloaddition of carbon dioxide and epoxides. *Chem. Sci.* **2017,** *8* (2), 1570-1575.

26. Zhao, M.; Ou, S.; Wu, C.-D., Porous Metal–Organic Frameworks for Heterogeneous Biomimetic Catalysis. *Acc. Chem. Res.* **2014,** *47* (4), 1199-1207.

27. Li, B.; Wen, H.-M.; Cui, Y.; Zhou, W.; Qian, G.; Chen, B., Emerging Multifunctional Metal–Organic Framework Materials. *Adv. Mater.* **2016,** *28* (40), 8819-8860.

28. Islamoglu, T.; Goswami, S.; Li, Z.; Howarth, A. J.; Farha, O. K.; Hupp, J. T., Postsynthetic Tuning of Metal–Organic Frameworks for Targeted Applications. *Acc. Chem. Res.* **2017,** *50* (4), 805-813.

29. Feng, X.; Song, Y.; Li, Z.; Kaufmann, M.; Pi, Y.; Chen, J. S.; Xu, Z.; Li, Z.; Wang, C.; Lin, W., Metal–Organic Framework Stabilizes a Low-Coordinate Iridium Complex for Catalytic Methane Borylation. *J. Am. Chem. Soc.* **2019,** *141* (28), 11196-11203.

30. Sawano, T.; Lin, Z.; Boures, D.; An, B.; Wang, C.; Lin, W., Metal–Organic Frameworks Stabilize Mono(phosphine)–Metal Complexes for Broad-Scope Catalytic Reactions. *J. Am. Chem. Soc.* **2016,** *138* (31), 9783-9786.

31. Lv, X.-L.; Wang, K.; Wang, B.; Su, J.; Zou, X.; Xie, Y.; Li, J.-R.; Zhou, H.-C., A Base-Resistant Metalloporphyrin Metal–Organic Framework for C–H Bond Halogenation. *J. Am. Chem. Soc.* **2017,** *139* (1), 211-217.

32. Cao, C.-C.; Chen, C.-X.; Wei, Z.-W.; Qiu, Q.-F.; Zhu, N.-X.; Xiong, Y.-Y.; Jiang, J.-J.; Wang, D.; Su, C.-Y., Catalysis through Dynamic Spacer Installation of Multivariate Functionalities in Metal–Organic Frameworks. *J. Am. Chem. Soc.* **2019,** *141* (6), 2589-2593.

33. Chen, C.-X.; Wei, Z.-W.; Pham, T.; Lan, P. C.; Zhang, L.; Forrest, K. A.; Chen, S.; Al-Enizi, A. M.; Nafady, A.; Su, C.-Y.; Ma, S., Nanospace Engineering of Metal–Organic Frameworks through Dynamic Spacer Installation of Multifunctionalities for Efficient Separation of Ethane from Ethane/Ethylene Mixtures. *Angew. Chem. Int. Ed.* **2021,** *60* (17), 9680-9685.

34. Hwang, Y. K.; Hong, D.-Y.; Chang, J.-S.; Jhung, S. H.; Seo, Y.-K.; Kim, J.; Vimont, A.; Daturi, M.; Serre, C.; Férey, G., Amine Grafting on Coordinatively Unsaturated Metal Centers of MOFs: Consequences for Catalysis and Metal Encapsulation. *Angew. Chem. Int. Ed.* **2008,** *47* (22), 4144-4148.

35. Yuan, S.; Chen, Y.-P.; Qin, J.-S.; Lu, W.; Zou, L.; Zhang, Q.; Wang, X.; Sun, X.; Zhou, H.-C., Linker Installation: Engineering Pore Environment with Precisely Placed Functionalities in Zirconium MOFs. *J. Am. Chem. Soc.* **2016,** *138* (28), 8912-8919.

36. Chang, G.-G.; Ma, X.-C.; Zhang, Y.-X.; Wang, L.-Y.; Tian, G.; Liu, J.-W.; Wu, J.; Hu, Z.-Y.; Yang, X.-Y.; Chen, B., Construction of Hierarchical Metal–Organic Frameworks by Competitive Coordination Strategy for Highly Efficient CO2 Conversion. *Adv. Mater.* **2019,** *31* (52), 1904969.

37. Zhou, W.; Huang, D.-D.; Wu, Y.-P.; Zhao, J.; Wu, T.; Zhang, J.; Li, D.-S.; Sun, C.; Feng, P.; Bu, X., Stable Hierarchical Bimetal–Organic Nanostructures as HighPerformance Electrocatalysts for the Oxygen Evolution Reaction. *Angew. Chem. Int. Ed.* **2019,** *58* (13), 4227-4231.

38. Wang, Y.; Jia, X.; Yang, H.; Wang, Y.; Chen, X.; Hong, A. N.; Li, J.; Bu, X.; Feng, P., A Strategy for Constructing Pore-Space-Partitioned MOFs with High Uptake Capacity for C2 Hydrocarbons and CO2. *Angew. Chem. Int. Ed.* **2020,** *59* (43), 19027-19030.

39. Lan, G.; Quan, Y.; Wang, M.; Nash, G. T.; You, E.; Song, Y.; Veroneau, S. S.; Jiang, X.; Lin, W., Metal–Organic Layers as Multifunctional Two-Dimensional Nanomaterials for Enhanced Photoredox Catalysis. *J. Am. Chem. Soc.* **2019,** *141* (40), 15767-15772.

40. Shi, W.; Quan, Y.; Lan, G.; Ni, K.; Song, Y.; Jiang, X.; Wang, C.; Lin, W., Bifunctional Metal–Organic Layers for Tandem Catalytic Transformations Using Molecular Oxygen and Carbon Dioxide. *J. Am. Chem. Soc.* **2021,** *143* (40), 16718-16724.

41. Fan, Y.; You, E.; Xu, Z.; Lin, W., A Substrate-Binding Metal–Organic Layer Selectively Catalyzes Photoredox Ene-Carbonyl Reductive Coupling Reactions. *J. Am. Chem. Soc.* **2021,** *143* (45), 18871-18876.

42. Cao, L.; Lin, Z.; Peng, F.; Wang, W.; Huang, R.; Wang, C.; Yan, J.; Liang, J.; Zhang, Z.; Zhang, T.; Long, L.; Sun, J.; Lin, W., Self-Supporting Metal–Organic Layers as Single-Site Solid Catalysts. *Angew. Chem. Int. Ed.* **2016,** *55* (16), 4962-4966.

43. Lan, G.; Ni, K.; Xu, R.; Lu, K.; Lin, Z.; Chan, C.; Lin, W., Nanoscale Metal–Organic Layers for Deeply Penetrating X-ray-Induced Photodynamic Therapy. *Angew. Chem. Int. Ed.* **2017,** *56* (40), 12102-12106.

44. Patil, D. V.; Yun, H.; Shin, S., Catalytic Cross-Coupling of Vinyl Golds with Diazonium Salts under Photoredox and Thermal Conditions. *Adv. Synth. Catal.* **2015,** *357* (12), 2622-2628.

45. Kim, S.; Rojas-Martin, J.; Toste, F. D., Visible light-mediated gold-catalysed carbon(sp2)–carbon(sp) cross-coupling. *Chem. Sci.* **2016,** *7* (1), 85-88.

46. Huang, L.; Rudolph, M.; Rominger, F.; Hashmi, A. S. K., Photosensitizer-Free Visible-Light-Mediated Gold-Catalyzed 1,2-Difunctionalization of Alkynes. *Angew. Chem. Int. Ed.* **2016,** *55* (15), 4808-4813.

47. Shu, X.-z.; Zhang, M.; He, Y.; Frei, H.; Toste, F. D., Dual Visible Light Photoredox and Gold-Catalyzed Arylative Ring Expansion. *J. Am. Chem. Soc.* **2014,** *136* (16), 5844-5847.

48. Marcoux, D.; Charette, A. B., Nickel-Catalyzed Synthesis of Phosphonium Salts from Aryl Halides and Triphenylphosphine. *Adv. Synth. Catal.* **2008,** *350* (18), 2967-2974.

49. Huang, L.; Rominger, F.; Rudolph, M.; Hashmi, A. S. K., A general access to organogold(iii) complexes by oxidative addition of diazonium salts. *Chem. Commun.* **2016,** *52* (38), 6435-6438.

50. Asomoza-Solís, E. O.; Rojas-Ocampo, J.; Toscano, R. A.; Porcel, S., Arenediazonium salts as electrophiles for the oxidative addition of gold(i). *Chem. Commun.* **2016,** *52* (45), 7295-7298.

51. Witzel, S.; Hoffmann, M.; Rudolph, M.; Rominger, F.; Dreuw, A.; Hashmi, A. S. K., A Radical Chain: Mononuclear "Gold Only" Photocatalysis. *Adv. Synth. Catal.* **2022,** *364* (3), 581-592.

52. Hashmi, A. S. K., Homogeneous Gold Catalysis Beyond Assumptions and Proposals—Characterized Intermediates. *Angew. Chem. Int. Ed.* **2010,** *49* (31), 5232-5241.

53. Lauterbach, T.; Asiri, A. M.; Hashmi, A. S. K., Chapter Five - Organometallic Intermediates of Gold Catalysis. In *Adv. Organomet. Chem.*, Pérez, P. J., Ed. Academic Press: 2014; Vol. 62, pp 261-297.

TOC Graphic